NTNU – Trondheim
Norwegian University of
Science and Technology

Radio Acoustic Sounding System for Wind Measurements

Andreas Hveding Øvstebø

Master of Science in Electronics
Submission date: June 2012
Supervisor: Jens F. Hjelmstad, IET
Co-supervisor: Ulf Kristiansen, IET

Norwegian University of Science and Technology
Department of Electronics and Telecommunications

Abstract

The objective of this assignment was to implement a bistatic radio acoustic sounding system (RASS) in a anechoic chamber, using equipment at hand. The purpose of which was to enable measurements within a controlled environment to avoid variations in wind, humidity and temperature. Radio acoustic sounding systems as well as planning of the test setups have been theoretically investigated in previous work.

The approach to the task has been to choose equipment assumed suitable for the experiment and verify the equipment suitability by measuring the technical characteristics relevant to the task. Then a bistatic RASS was constructed within a anechoic chamber. Using software defined radios, the received signals were digitally sampled. So was the acoustic field in the volume of interaction.

Although processing the results failed to detect any sign of scatter, the equipment has been thoroughly tested. The acoustic, as well as electromagnetic equipment have shown good results with respect to the suitability for such a system prototype.

No conclusion as to whether any scattering occurs as a consequence of the acoustic field can be made, as the absence of such indications may merely indicate insufficient sending power or too high levels of background noise. Prior to these findings, the equipment were concluded to be suitable for a prototype bistatic RASS. Methods to improve the measurement quality have been suggested as future work.

Sammendrag

Målet med denne masteroppgaven var å implementere et bistatisk radioakustisk sonderingssystem (RASS) i et ekkofritt rom ved hjelp av tilgjengelig utstyr. Hensikten var å muliggjøre målinger i et kontrollert miljø for å unngå variasjoner i vind, luftfuktighet og temperatur. Selve RASS-konseptet har blitt teoretisk undersøkt i et tidligere arbeid.

Tilnærmingen til oppgaven har vært å først gjøre en enkel studie av utstyret ment for forsøket for å kartlegge de tekniske egenskapene relevante for senere målinger. Deretter har en bistatisk RASS blitt konstruert. Gjennom bruk av programmerbare radioenheter og lydopptakere har alle signalene blitt punktprøvd og lagret digitalt.

Resultatene viste ingen korrelasjon mellom det akustiske og det elektromagnetiske signalet. Til tross for dette har det akustiske og elektromagnetiske utstyret vist seg godt egnet til å basere en RASS prototype på, spesielt med tanke på brukervennlighet i forbindelse med hurtige endringer i parametre.

Det er ikke mulig å konkludere hvorvidt refleksjon av elektromagnetiske bølger finner sted i det akustiske feltet, da årsaken kan ligge i utilstrekkelig sendereffekt, akustisk eller elektromagnetisk. Før målingene på RASS prototypen ble det konkludert at det akustiske, såvel som det elektromagnetiske utstyret var egnet for en bistatisk RASS. Konkrete forslag til forbedringer av systemet har blitt foreslått.

Contents

1 Introduction **1**
- 1.1 Background . . . 1
- 1.2 Problem Description and Thesis Overview . . . 1

2 Theory **2**
- 2.1 Introduction to Radio Acoustic sounding Systems (RASS) . . . 2
- 2.2 RASS applied to Measurement of Wind . . . 2
- 2.3 Bragg Scatter . . . 2
- 2.4 Reflection at a Bragg Surface . . . 3
- 2.5 Doppler Shifts due to forward Scatter . . . 3
- 2.6 Attenuation of Sound in the Atmosphere . . . 3

3 Ettus Research USRP2 **5**
- 3.1 GNU Radio and GNU Radio Companion . . . 5
- 3.2 USRP2 and GNU Radio Companion . . . 6

4 Calculations **7**
- 4.1 Bragg matching of a incident Wave at an Angle . . . 7
- 4.2 Reflection at a Bragg Surface . . . 7
- 4.3 Calculation of Doppler Shifts . . . 8
- 4.4 Absorption in Air . . . 8

5 Equipment used **10**
- 5.1 Computer Hardware and Software . . . 10

6 Measurement Methodology **12**
- 6.1 Equipment Verification . . . 12
  - 6.1.1 Acoustic Equipment . . . 12
  - 6.1.2 Radio Equipment . . . 12
- 6.2 Bistatic RASS . . . 13
  - 6.2.1 Setup A . . . 15
  - 6.2.2 Setup B . . . 15
  - 6.2.3 Acoustic and Electromagnetic Observations . . . 15

7 Results **21**
- 7.1 Equipment Verification . . . 21
  - 7.1.1 Power Amplifier and acoustic Source . . . 21
  - 7.1.2 Measurement- and recording Chain . . . 21

7.1.3 Radio Equipment . . . 21
7.2 Bistatic RASS . . . 21
7.2.1 Bistatic RASS, Setups A and B . . . 21
7.2.2 Acoustic and Electromagnetic Observations . . . 22

8 Discussion **38**
8.1 Equipment Verification . . . 38
8.1.1 Acoustic Equipment . . . 38
8.1.2 Radio Equipment . . . 38
8.2 Bistatic RASS . . . 38
8.2.1 Acoustic and Electromagnetic Observations . . . 39
8.3 The System in conjunction with meteorological Measurements . . . 39

9 Improvements to the Test Setup (Future work) **40**
9.1 Connecting Radios and acoustic Source . . . 40
9.2 Enhancing acoustic Power and using Frequency Sweeps . . . 40
9.2.1 Enhancing Radio transmitting Power and reduce direct Transmission . . . 41

10 Conclusions **43**
10.1 Equipment verification . . . 43
10.2 Bistatic RASS . . . 43

References **45**

A Abbreviations and Definitions **46**

B Matlab Scripts **48**

C Horn Antennas used **52**

List of Figures

1 USRP2 with horn antenna . . . 5
2 Absorption in air . . . 9
3 Acoustic connections . . . 14
4 USRP2 connections . . . 14
5 Transmitter block diagram . . . 16
6 Receiver block diagram . . . 17

7 Bistatic RASS, picture . . . 18
8 Setup A 2D Sketch . . . 18
9 Setup A 3D Sketch . . . 19
10 Setup B 2D Sketch . . . 20
11 Acoustic acoustic source, frequency response . . . 23
12 Acoustic acoustic source, beaming @ 12.5kHz . . . 24
13 Acoustic acoustic source, beaming @ 20.5kHz . . . 24
14 Brüel & Kjær Type 4939 microphone . . . 25
15 USRP2 receiving noise . . . 26
16 USRP2 receiving a signal . . . 26
17 USRP2 receiving with horn antenna . . . 26
18 Received signal in time domain (A) . . . 27
19 Received signal spectrogram (A) . . . 28
20 Received signal spectrogram (A) . . . 29
21 Mean FT plot (A) . . . 30
22 Received signal in time domain (B) . . . 31
23 Received signal spectrogram (B) . . . 32
24 Received signal spectrogram (A) . . . 33
25 Mean FT plot (A) . . . 34
26 Gliding RMS, 20.6kHz . . . 35
27 Gliding RMS, 12.8kHz . . . 36
28 Frequency drift on radios . . . 37
29 Matlab: computeSpectrogram100ksRelative.m . . . 48
30 Matlab: readFileGetFreqlevels.m . . . 49
31 Matlab: makePolarPlots.m . . . 50
32 Matlab: computeGlidingRMS.m . . . 51
33 Horn antennas: Polar diagram . . . 52

List of Tables

1 USRP2 technical specifications . . . 6
2 Equipment used . . . 10
3 Computer specifications . . . 11
4 List of abbreviations . . . 46
5 List of definitions . . . 47

1 Introduction

1.1 Background

During the last decades the public, as well as scientific communities have realized the need for a change towards a more environmentally friendly society. With the increased knowledge, the willingness to pay for environmentally friendly solutions is increasing [1]. Windpower is, among other renewable energy sources, a growing industry.

For high accuracy wind profiling in conjuncture with windpower plants, various methods are in use involving RADAR systems. One limitation of such a system is the need for turbulent flow for sufficient forward scatter of the electromagnetic wave, which requires a sufficiently high wind velocity. At low wind velocities the wind flow tend to be laminar, excluding the use of such a system for measurements. Inducing an acoustic field for forward scattering the waves have proven successful in other meteorological appliances [2] and may prove useful also for this appliance. Such a system is called a radio acoustic sounding system (RASS).

1.2 Problem Description and Thesis Overview

The thesis aims to execute an experiment in which a downsized radio acoustic sounding system is to be constructed. Improvements to the system, with respect to wind measurements in conjunction with windpower and meteorological measurements, are to be considered, based on the results.

The RASS described in this thesis is based on previous work done by the author and Triad AS[3][4][5].

The thesis consist of a brief introduction to the basic mechanisms involved in a RASS, the complete specifications on how it was constructed, a description of the method of measurement, a discussion including suggestions for future work and conclusions. As the author failed to detect any forward scatter from the acoustic disturbance on this system, future RASS should be made according to the suggestions for improvement in order to produce any measurable scatter at all.

2 Theory

2.1 Introduction to Radio Acoustic sounding Systems (RASS)

The basic idea of Radio Acoustic Sounding Systems, RASS, has been around for many years. The earliest demonstration of a RADAR using scattering by sound waves took place in 1961, and scattering of light acoustically has been known at least since 1932[6]. The principal mechanism behind a RASS is that an acoustic disturbance yields a proportional disturbance in electric permittivity, ϵ. Any transition between media of different permittivity will reflect electromagnetic waves[7][4].

2.2 RASS applied to Measurement of Wind

The propagating speed of an acoustic disturbance relies upon several material-specific parameters such as density, humidity, temperature and elasticity[8]. If the media, in which the sound wave propagates, itself is moving, this will also contribute to the total speed of the sound wave. Thus it follows that a radio acoustical sounding system can measure the movements of the air[4].

2.3 Bragg Scatter

Assume parallel reflective surfaces, in a periodic pattern with a fixed distance between them. These surfaces will both reflect and transmit the energy of a incident wave, passing the transmitted energy to the next surface. It follows that the total energy reflected in such a structure will consist of contributions from all the surfaces. To achieve maximum power of this reflection, all contributions should be in phase, yielding

$$n\lambda = 2d \tag{2.1}$$

which is known as the Bragg condition. n could be any natural number, including 1, λ is the wavelength and d is the distance between the reflective surfaces. When applied in a RASS, the acoustic disturbance can be treated as such a periodically layered structure, with a minor alternation to the condition. The reflection is phase shifted 180° when the initial wave passes to a material of higher refractive index. As a result, Bragg matching occurs only for $n = 1$, yielding the Bragg condition for radio acoustic interaction

$$\lambda_{EM} = 2\lambda_{Ac} \tag{2.2}$$

with λ_{EM} and λ_{Ac} being the parallel electromagnetic and acoustic wavelengths, respectively[9]. If $\lambda_{EM} \nparallel \lambda_{Ac}$, then a Bragg match requires $\lambda_{EM}^{\parallel \lambda_{Ac}}$ to satisfy the Bragg criteria[5]. The Bragg condition for a bistatic RASS is then

$$\lambda_{EM} \cos\theta = 2\lambda_{Ac} \tag{2.3}$$

with θ being the angle of incidence, $\theta = \angle\{\vec{k}_{EM}, \vec{k}_{Ac}\}$.

2.4 Reflection at a Bragg Surface

[4] provides the following relation between the acoustic source and the electromagnetic scattering

$$\vec{E_S} = (\vec{E} * \frac{dp}{P_{atm}})(\vec{r}) \tag{2.4}$$

with $\vec{E_S}$ being the forward scatter of the electric field, $E(\vec{r})$ and dp being the difference from atmospheric pressure, P_{atm}. Equation 2.4 yields directly that the magnitude of the scattering is both proportional to the EM-source and the acoustic source.

If the reflected power is insufficient for a reliable detection of a reflection, one could either increase the number of acoustic waves per pulse or the intensity of the acoustic source[9]. Remark that the total usable amount of acoustic wavelengths are dependent on the volume created by the antennae beamwidths, and that longer pulses beyond will only yield longer, not more powerful, reflected EM-pulses[5].

2.5 Doppler Shifts due to forward Scatter

The doppler shift, f_d, in the forward scattered signal is

$$f_d = f_a \tag{2.5}$$

where f_a is the acoustic frequency[9].

2.6 Attenuation of Sound in the Atmosphere

The intensity of the electromagnetic scatter in a RASS depends largely on the intensity of the acoustic disturbance in the point of interaction. The sound pressure amplitude of a plane wave will decrease exponentially, due to attenuation, as it travels over a distance s, and will follow the formula

$$P_s = P_0 e^{-\alpha s} \tag{2.6}$$

where P_0 is the initial sound pressure amplitude and P_s is the pressure amplitude in s. The absorption coefficient, α, may be approximated with the formula

$$\alpha_S \approxeq \frac{1}{2}\frac{2\pi f}{c_{Ac}} 2\pi f \tau_S \tag{2.7}$$

with f being the frequency. This approximation is only valid for $2\pi f \tau_S << 1$, and the relaxation time in air, τ_S can be assumed to be $10^{-10} s$[10].

3 Ettus Research USRP2

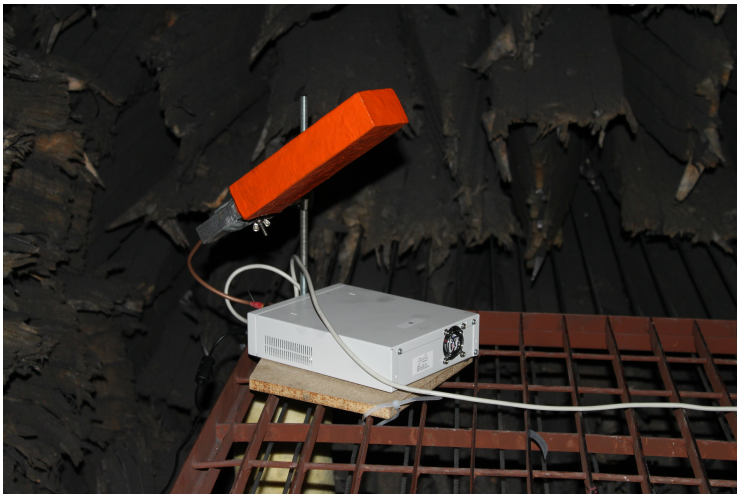

Figure 1: *Ettus Research USRP2 with a horn antenna mounted on a custom made antenna stand.*

The Ettus Research USRP2 is a software defined radio platform, specially designed for prototyping radio systems. The two radios used were equipped with XCVR2450 transceiver daughter boards, suitable for transmitting and receiving at $4.9 - 5.9GHz$. The main technical specifications are listed in table 3. More information on USRP2 can be found on [11].

3.1 GNU Radio and GNU Radio Companion

GNU Radio is a toolkit consisting of signal processing blocks to be used with various external radio-frequency hardware. GNU Radio Companion (GRC) is a graphic front end for GNU Radio, allowing radio systems to be programmed graphically in very little time by connecting various blocks of functionality to form more complex systems.

Table 1: *Technical specifications on the Ettus Research USRP2 and the XCVR2450 transceiver daughter board equipped.*

Ettus Research USRP2	
Hardware version	4.0
Computer interface	Gigabit Ethernet
XCVR2450 Transceiver	
Maximum transmitting power @ $2.4 - 2.5GHz$	$100mW$
Maximum transmitting power @ $4.9 - 5.9GHz$	$50mW$
Antenna output impedance	50Ω

3.2 USRP2 and GNU Radio Companion

The USRP2 can easily be included in a GNU Radio system by adding the USRP2 block in an open GRC window, and connect the computer to the radio by ethernet. This provides the user with a fully operational and customizable radio transceiver. The transceiver has the ability to do most signal processing prior to transmitting or after receiving, digitally with pre-programmed signal processing blocks.

The advantages of using such a system in a bistatic RASS are many. Firstly, one can quickly design, implement and test a system without having to do any re-wiring or circuit design. This allows for the user to concentrate on the task at hand on a system level. Also, the USRP2 features mixers, amplifiers and signal paths within one box, meaning the user never have to consider which parts are compliant.

The are also some disadvantages to the use of a software defined radio in a measurement setup. Due to high level control, it is hard to know at all times the exact physical parameters, such as voltages or currents. All measured samples are relative and unit-less. Also, the gain and transmitting power is limited by the output stage and receiver circuit.

4 Calculations

4.1 Bragg matching of a incident Wave at an Angle

The two measurement setups, setup A and B, specify different locations for radio equipment, affecting the angle of incidence on the acoustic field (Figures 8 and 10). More specifically, the angles of incidence are

$$\theta_A = \arctan\left\{\frac{3.0m}{2.0m}\right\} = 56.3\,^\circ \tag{4.1}$$

$$\theta_B = \arctan\left\{\frac{1.0m}{2.0m}\right\} = 26.5\,^\circ \tag{4.2}$$

$$\tag{4.3}$$

The Bragg criteria for a RASS is defined in equation 2.3. Choosing the frequency of the electromagnetic wave to be $f_{EM} = 5GHz$ and assuming the speed of light to be $c_{EM} = 299792458\frac{m}{s}$ and the speed of sound to be $c_{Ac} = 343.2\frac{m}{s}$ yield the following Bragg matched parameters

$$\lambda_{EM} = \frac{c_{EM}}{f_{EM}} = 60mm$$

$$\lambda_{Ac,A} = \frac{\lambda_{EM}}{2}\cos\theta_A = 16.6mm$$

$$\lambda_{Ac,B} = \frac{\lambda_{EM}}{2}\cos\theta_B = 26.8mm$$

$$\Downarrow$$

$$f_{Ac,A} = \frac{c_{Ac}}{\lambda_{Ac,A}} = 20.64kHz \tag{4.4}$$

$$f_{Ac,B} = \frac{c_{Ac}}{\lambda_{Ac,B}} = 12.8kHz \tag{4.5}$$

4.2 Reflection at a Bragg Surface

2.4 provides following relation between the acoustic source and the electromagnetic scattering

$$\vec{E_S} = E(\vec{r}) * \frac{dp}{P_{atm}}(\vec{r}) \tag{4.6}$$

with $\vec{E_S}$ being the forward scatter of the electric field $E(\vec{r})$ and dp being the difference from atmospheric pressure, P_{atm}. The equation yields directly that

the scattered signal must be proportional to both the acoustic and the electromagnetic source.

4.3 Calculation of Doppler Shifts

The Doppler shifts, f_d, introduced by the acoustic wave are

$$f_d = f_a \tag{4.7}$$

with f_a being the acoustic frequency. The expected Doppler shifts are then $20640Hz$ and $12800Hz$ for setup A and B, respectively. Taking into account that the receiver (figure 6) mixes the received signal to approximately $-20kHz$, the observed forward scatter should occur at approximately $40.6kHz$ and $32.8kHz$.

4.4 Absorption in Air

Using the approximation for the atmospheric absorption,

$$\alpha_S = \frac{1}{2}\frac{\omega}{c_{Ac}}\omega\tau_S \tag{4.8}$$

and assuming the following parameters

$$\begin{aligned} \tau_S &= 10^{-10}s \\ c_{Ac} &= 343.2m/s \end{aligned}$$

yields $\alpha_S = 942.33 \cdot 10^{-6}m^{-1}$ and $\alpha_S = 2450.20 \cdot 10^{-6}m^{-1}$ for $12.8kHz$ and $20.64kHz$ respectively. The normalized amplitude due to absorption, $e^{-\alpha_S r}$, is then obtained and plotted for $r \in (0, 4)m$ (figure 2).

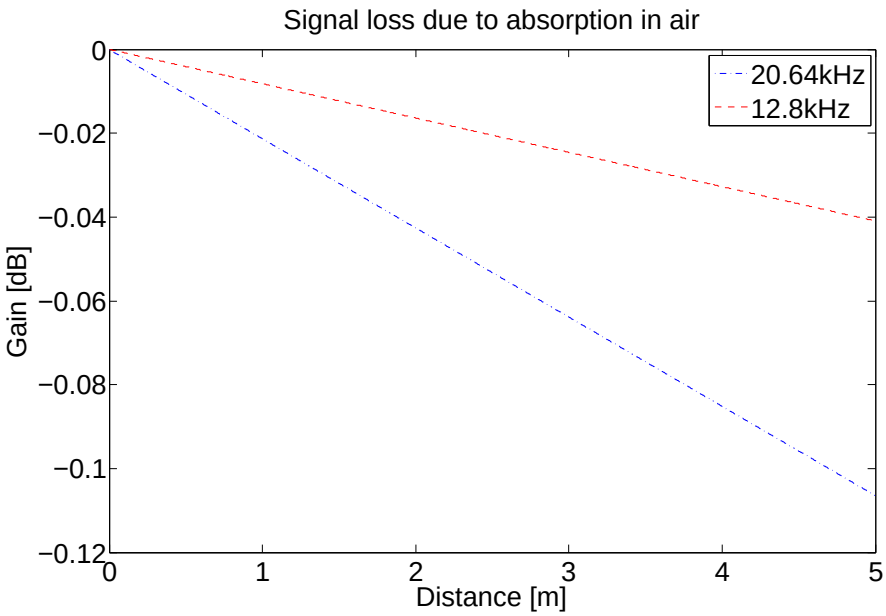

Figure 2: *The signal loss due to atmospheric absorption in air.*

5 Equipment used

Table 2: *All active equipment used for the measurements. Some equipments lacked proper serial numbers and have been marked *. These equipments have been noted with university inventory numbers or week of production.*

Item	Make and Model	Serial number
Microphone	Brüel & Kjær Type 4939	2546543
Mic. pre-amplifier	Norsonic 1201	30517
Mic. amplifier	Norsonic 336	20626
Mic. calibrator	Brüel & Kjær Type 4230	1719650
HD recorder	Sound Devices 722	470305025004
Oscilloscope	Kenwood CS-5135	9110132
Acoustic source	Seas H0615 - 25 TFFN/G	Week 19/00*
Power amplifier	Crown DC300	CB-4059*
Function generator	Wavetek 178	AC6590409
Radio transmitter	Ettus Research USRP2 ver. 4.0	1146
Radio receiver	Ettus Research USRP2 ver. 4.0	1153
Transmitter antenna	Horn antenna, 4-8GHz	A4-8:2*
Receiver antenna	Horn antenna, 4-8GHz	A4-8:1*
Transmitter PC	Lenovo 2847	LR-KWNMT 10/08
Receiver PC	Lenovo 2847	LR-KWNME 10/08
Still Camera	Canon EOS 500D	1550527658

5.1 Computer Hardware and Software

The computers used with the USRP2s are part of the USRP2 lab and their specifications is listed in table 5.1.

Table 3: *Technical specifications on the computers used with the USRP2s.*

Lenovo 2847 USRP2 Controller computers	
Operating system	Ubuntu Release 10.04
Linux Kernel	Linux 2.6.32-41 Generic
Graphical user interface	GNOME 2.30.2
GNU Radio Companion	Ver. 3.3.0
Processor	Intel Core2 Duo T6570
CPU Clock speed	$2.10GHz$
Number of cores	2
Physical memory (RAM)	$1.8GiB$

6 Measurement Methodology

6.1 Equipment Verification

Before setting up a complete RASS in the anechoic chamber, two minor studies were made of the equipment intended used. The purpose of these was to get to know the equipment's limitations and reducing time spent in the anechoic chamber.

6.1.1 Acoustic Equipment

A short study was made to conclude on what acoustic equipment were suitable for the RASS experiments described in 6.2.1 and 6.2.2. A $\frac{1}{4}''$ microphone and a $SeasH061525TFFN/G$ tweeter as acoustic source were used. Both the frequency response and the directivity of the acoustic source were tested.

The characterization of the acoustic equipment was done in the anechoic chamber at NTNU, during the period February 20th-27th All measurements were made at $\approx 17°C$.

1. With acoustic source connected, the power amplifier output voltage was measured with oscilloscope for frequencies $100 - 40000Hz$.
2. The function generator (figure 3) was replaced by a computer.
3. The acoustic source was placed on a turntable, and the microphone placed directly in front of it.
4. Using WinMLS, the frequency response was measured with 10° intervals, from $-90°$ to $90°$.
5. Exporting the frequency responses to Matlab work space, the data was converted to polar plots with the script `makePolarPlots.m`.

6.1.2 Radio Equipment

Ettus Research's USRP2 software defined radios were chosen for the ease of altering frequencies and digitally recording signals. A short study was made to verify the software defined radios functionality. The characterization of the radio equipment was done in a computer lab at NTNU, during the period April 1st-12th. The measurements were made after work hours to reduce the EM-noise. All measurements were made in room temperature i.e. $\approx 20°C$.

1. The 2 USRP2s were connected to 2 computers by ethernet according to figure 4.

2. A simple receiver, consisting of a USRP2 source, a filter and a FFT were made in Gnu Radio Companion. The receiving USRP2 had a center frequency of $5GHz$.

3. A simple transmitter, consisting of a USRP2 sink connected to a fixed number input were made in Gnu Radio Companion. The USRP2 transmitted at $5.0003GHz$.

4. The two programs were run simultaneously.

5. The real time FFT plot was studied to find background noise and signal to noise ratio.

6. The antennas were replaced by horn antennas and the real time FFT plot was studied to find background noise and signal to noise ratio.

6.2 Bistatic RASS

The measurements of the RASS were conducted with two slightly different setups. Both setups feature bistatic RASS measured in a anechoic chamber. The difference between the two setups is the distance between the radio antennas, and therefore the angle of incidence into the acoustic field. The measurements were made during the period May 12th-20th at $\approx 17°C$.

1. The equipment was placed according to figure 8 for setup A, figure 10 for setup B, and connected according to figures 3 and 4. The output of the power amplifier was set to $38.5V_{P-P} = 13.6V_{RMS}$.

2. The function generator was set on *burstmode* with frequency $20640Hz$ for setup A, $12400Hz$ for setup B. Burst length was set to $1s$, that is $20640periods$ and $12400periods$ for setup A and B, respectively.

3. The block diagrams, figures 5 and 6, were loaded into the USRPs, and executed.

4. The file output from the receiver computer was then saved.

The sampled data was then processed using Matlab as follows

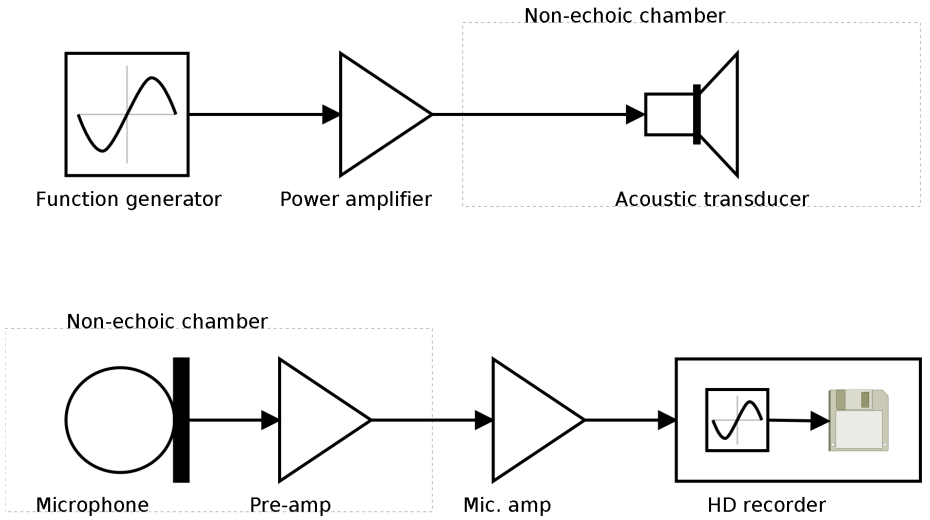

Figure 3: *Acoustic connections.*

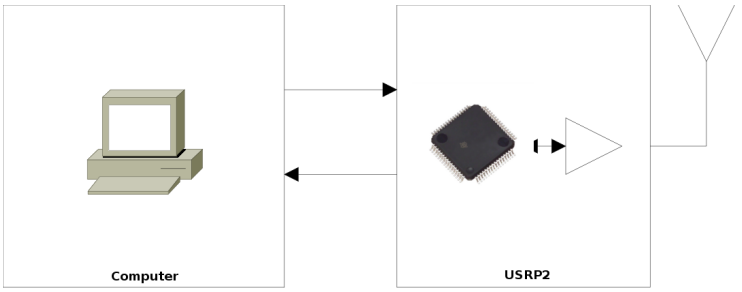

Figure 4: *USRP2 connections.*

1. The output files were read into Matlab workspace with the built in functions `fopen()` and `fread()`.

2. Using the self made function `computeSpectrogram.m`, the spectrogram was computed and plotted. The spectrograms were computed both as relative spectrograms (compared to the mean FFT) and as absolute spectrograms. The mean FFTs were also computed.

3. Using the self made function `computeGlidingRMS.m`, the time varying RMS values were computed (un-calibrated).

The usage of spectrograms was suggested by Brooker and Martinez[9].

The radio transmitter and receiver block diagrams are depicted in figures 5 and 6, and are identical to the ones used in 6.2.2. $5GHz$ was chosen for carrier frequency because it is just below the highest frequency on which the radios can operate. Receiving on $5GHz$ baseband, the receiver then feeds the signal through a mixer, a decimating filter and into a file sink. The mixer is designed (and tuned) to shift the signal from $-300kHz$ to $+22kHz$, allowing for $\geqslant 21kHz$ Doppler shifts in both directions when limited to $50kHz$ bandwidth when sampling at $100kHz$.

6.2.1 Setup A

This setup makes maximum use of the size of the anechoic chamber by placing the acoustic source in the centre of the room, and the antennas in opposite corners (figure 9). The distance between antennas are $6.0m$, and the acoustic source is placed directly between them, pointing upwards. Both the antennas and acoustic source point towards a point $2.0m$ directly above the acoustic source.

6.2.2 Setup B

In this setup the acoustic source is placed in the centre of the room, with the antennas placed symmetrically on opposite sides of it with $2.0m$ between them. The point of interest is still $2.0m$ directly above the acoustic source, reducing the angle of incidence (equation 4.1). This reduces the power of direct travelling radio waves from one antenna to the other, as the antennas are directional (Figure 33).

6.2.3 Acoustic and Electromagnetic Observations

While measuring with the USRP2 radios, acoustic signals were also recorded in WAV format (Standard pulse code modulation). The recording chain was calibrated, allowing for calibrated recordings of the acoustic field where reflection was assumed to occur. Calibrated RMS values were then computed with the Matlab function `computeGlidingRMS.m`.

Also, the quality of the directly transmitted carrier was investigated by zooming in on the spectrograms to uncover any frequency drift.

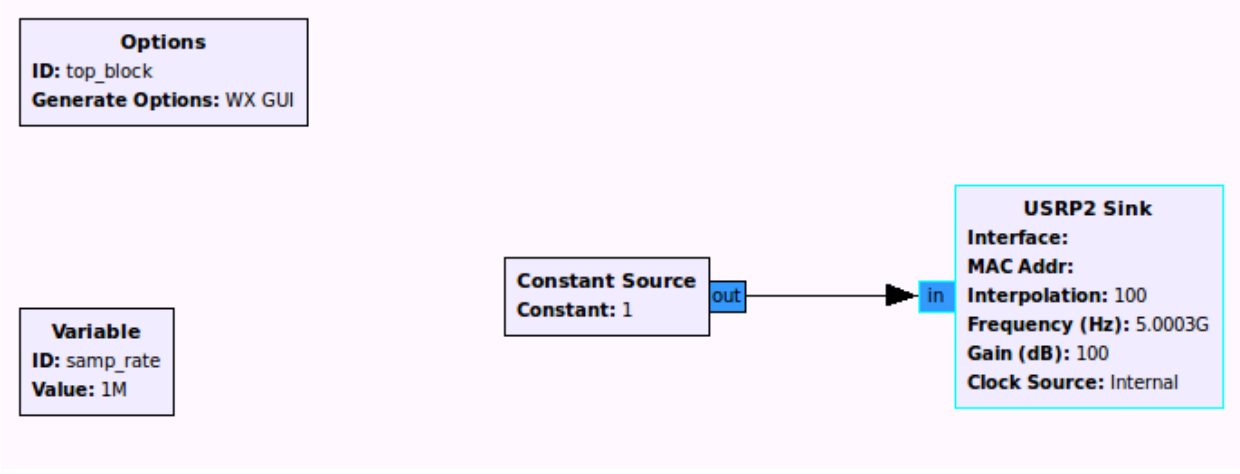

Figure 5: *Block diagram of the radio transmitter.*

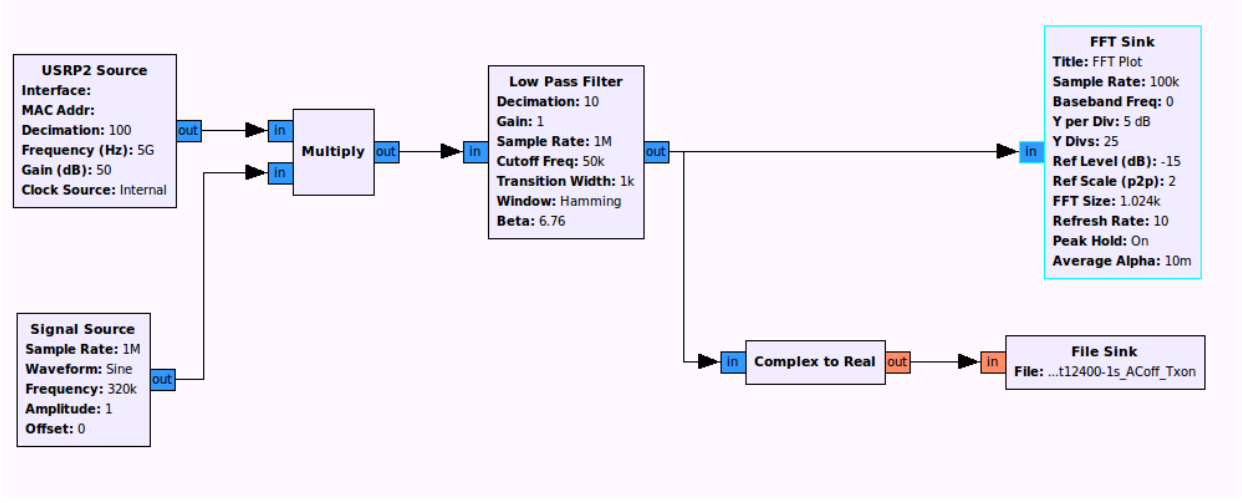

Figure 6: *Block diagram of the radio receiver.*

Figure 7: *An image composed of three pictures, showing the entire bistatic RASS, setup A in the anechoic chamber.*

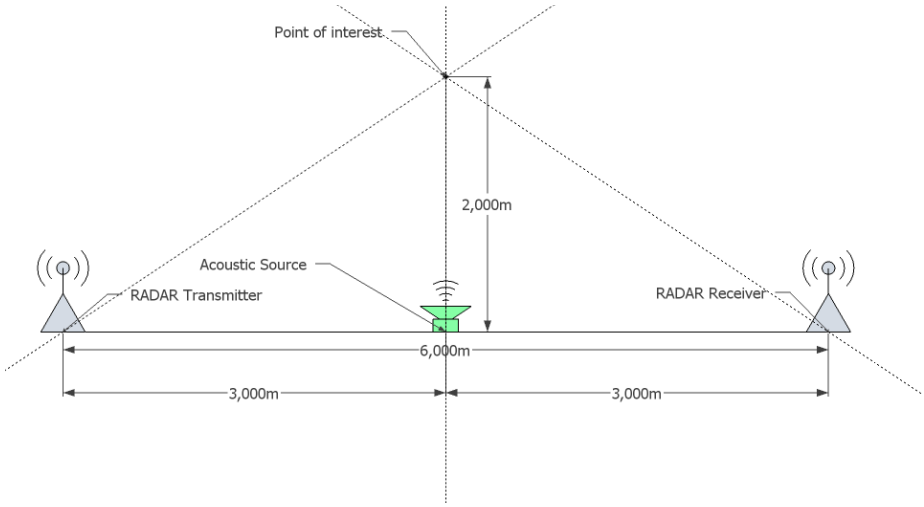

Figure 8: *Setup A. Sketch of antenna and acoustic source placements in the anechoic chamber.*

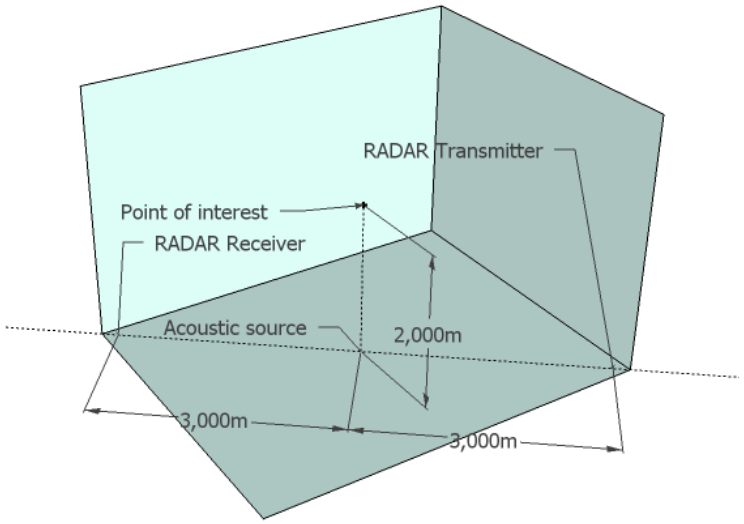

Figure 9: *Setup A. Sketch of antenna and acoustic source placements in the anechoic chamber.*

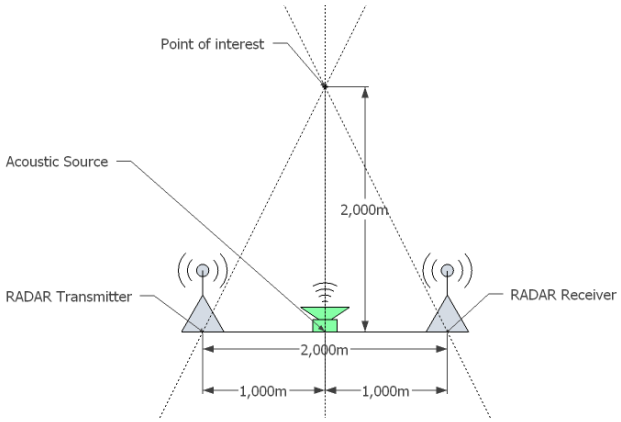

Figure 10: *Setup B. Sketch of antenna and acoustic source placements in the anechoic chamber.*

7 Results

7.1 Equipment Verification

7.1.1 Power Amplifier and acoustic Source

The power amplifier output voltage was measured, with oscilloscope, to be $38.5V_{P-P}$ for all frequencies in the range $100 - 40000Hz$. Thus the gate voltage at the acoustic source can be said to be constant for all frequencies in the range $100 - 40000Hz$. The acoustic source frequency response on axis reveals on axis power transmitted to be within $10dB$ for the frequencies $10k - 30kHz$ and within $6dB$ at $10k - 21kHz$ (Figure 11). The acoustic source has a beam width well below $30\,^\circ$ at $20.5hHz$ and the relative level is below $-20dB$ at $60\,^\circ$ off axis (Figure 13).

7.1.2 Measurement- and recording Chain

The microphone used, has a frequency response variation within $1dB$ in the frequency area $100 - 50000Hz$ (Figure 14). For recording sampled sound a hard drive recorder was used, recording at $96.1ksps/24bps$, ensuring a bandwidth of $48kHz$ according to the Nyquist theorem (Appendix A). The frequency response on the recorder is specified to be within $1dB$ in the frequency range $10 - 40000Hz$[12].

Combining the variations in frequency response, a total variation of less than $2dB$ can be expected for the whole acoustic measurement- and recording chain for all frequencies $100 - 40000Hz$.

7.1.3 Radio Equipment

Comparing the two FFTs, figures 15 and 16, it is apparent that the signal to noise ratio is approximately $24dB$. After setting up the radios, establishing contact and measuring the received power, the antennas were replaced by horn antennas. When replacing both antennas by directive horn antennas (Figure 17), the SNR was $\approx 40dB$.

7.2 Bistatic RASS

7.2.1 Bistatic RASS, Setups A and B

Studying figures 19 and 23 one can clearly see the direct transmission at approximately $22kHz$. Since the acoustic source is toggled with a burst time of

$1s$, any effect on the received signal should in some way correlate to this burst pattern. Visually studying the spectrograms at hand yields no indication of any periodic disturbance.

When comparing the differential spectrogram (figures 20 and 24) to the spectrogram, one may notice that although the overall noise have been reduced, the peak at around $22kHz$ is still present. It is still not possible to visually detect any periodic disturbance that correlates with the acoustic bursts of $1s$ length.

The time varying RMS plots (figures 18 and 22) show no visual indication of any $1s$ long bursts in RMS.

7.2.2 Acoustic and Electromagnetic Observations

The acoustic effective sound pressures (figures 18 and 22) were $0.4Pa$@$20.6kHz$ and $1.3Pa$@$12.8kHz$ in the area of interaction, thus the SPLs were $86dB$@$20.6kHz$ and $96.3dB$@$12.8kHz$.

When computing the spectrograms in 7.2.1, it was discovered that the frequency of the received peak varies with time. This can be seen in figure 28. It is also apparent that there is a difference in $\approx 2kHz$ when comparing transmitter settings, digital signal path and received signal.

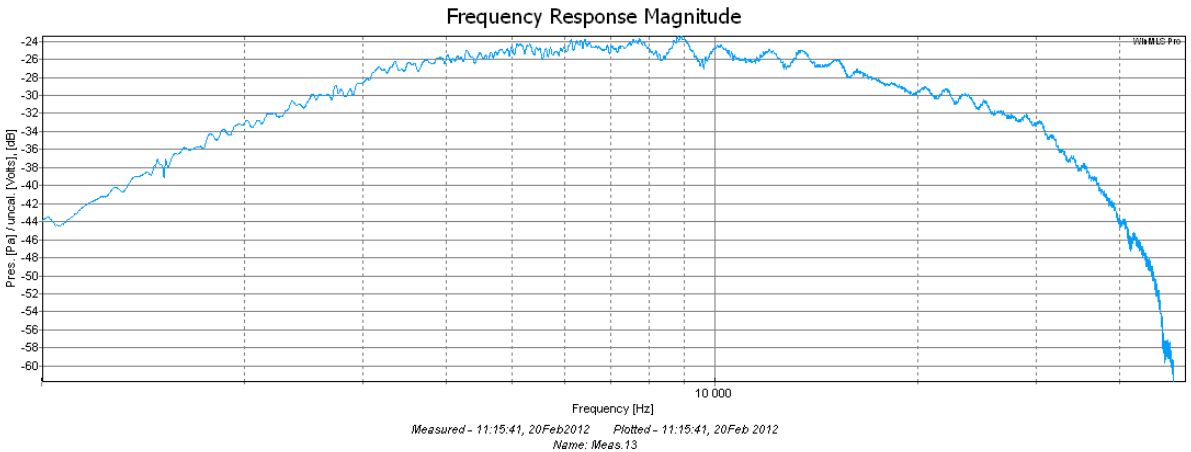

Figure 11: *The relative frequency response of the acoustic source, measured and plotted with the software WinMLS.*

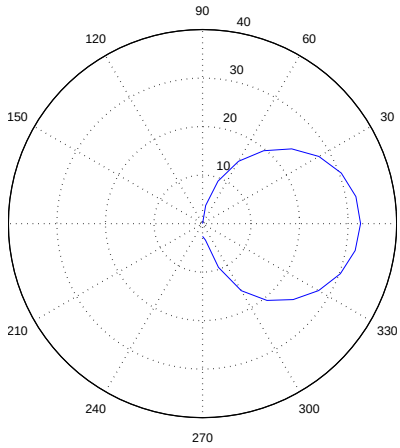

Figure 12: *The beaming properties of the acoustic source at* $12.5kHz$*, in relative dB as a function of angle in degrees. Automatically computed in Matlab, based on data measured with WinMLS.*

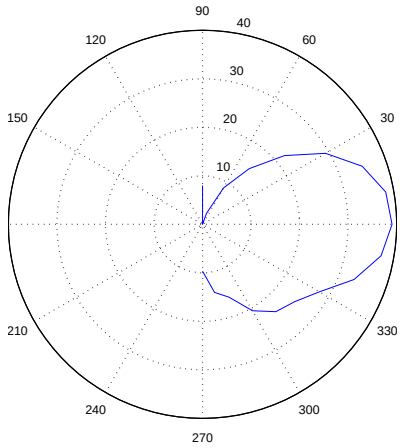

Figure 13: *The beaming properties of the acoustic source at* $20.5kHz$*, in relative dB as a function of angle in degrees. Automatically computed in Matlab, based on data measured with WinMLS.*

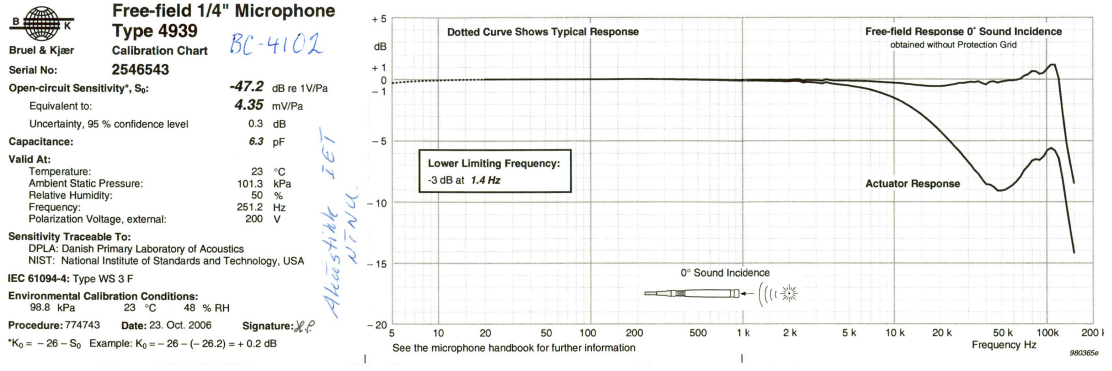

Figure 14: *Data sheet of the microphone used, a Brüel & Kjær Type 4939 free field microphone.*

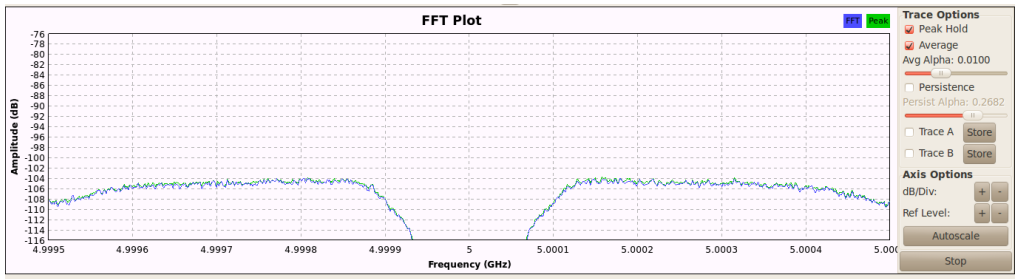

Figure 15: *FFT of received signal when not transmitting anything. Simple dipole antenna used.*

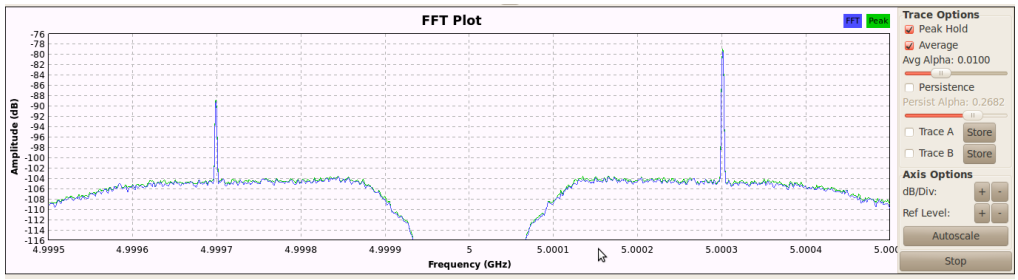

Figure 16: *FFT of received signal when transmitting at 5.0003GHz on another USRP2. Simple dipole antenna used.*

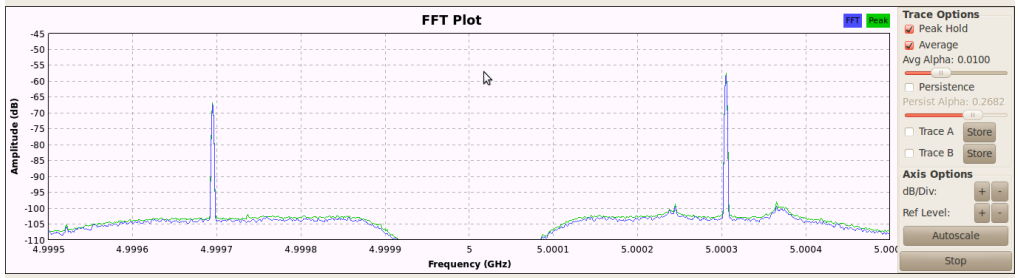

Figure 17: *FFT of received signal when transmitting at 5.0003GHz on another USRP2. Horn antenna used on both Tx and Rx.*

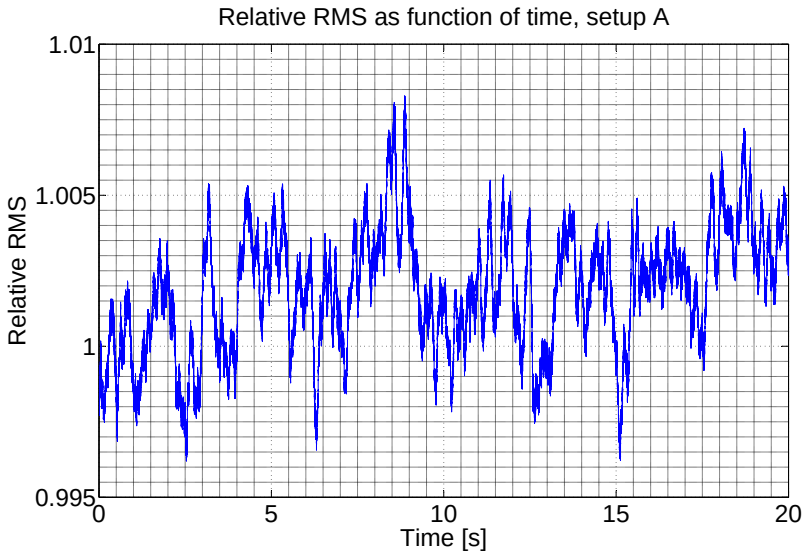

Figure 18: *Plot of the received signal's RMS in time domain. No signs of* $1s$ *long periodic disturbances of any kind.*

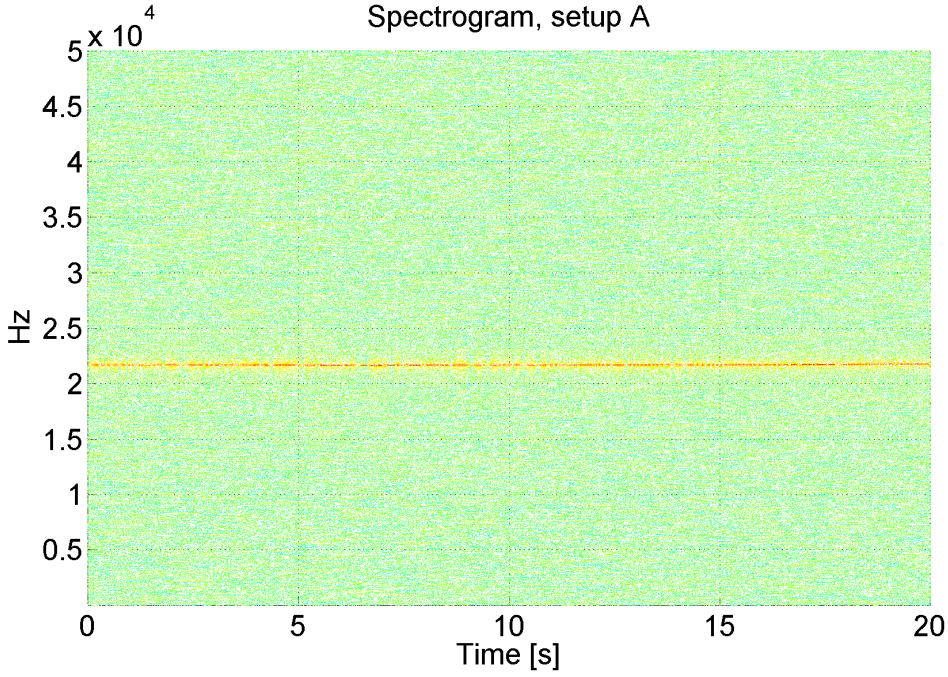

Figure 19: *Spectrogram of the received signal. No signs of* 1*s long periodic disturbances of any kind.*

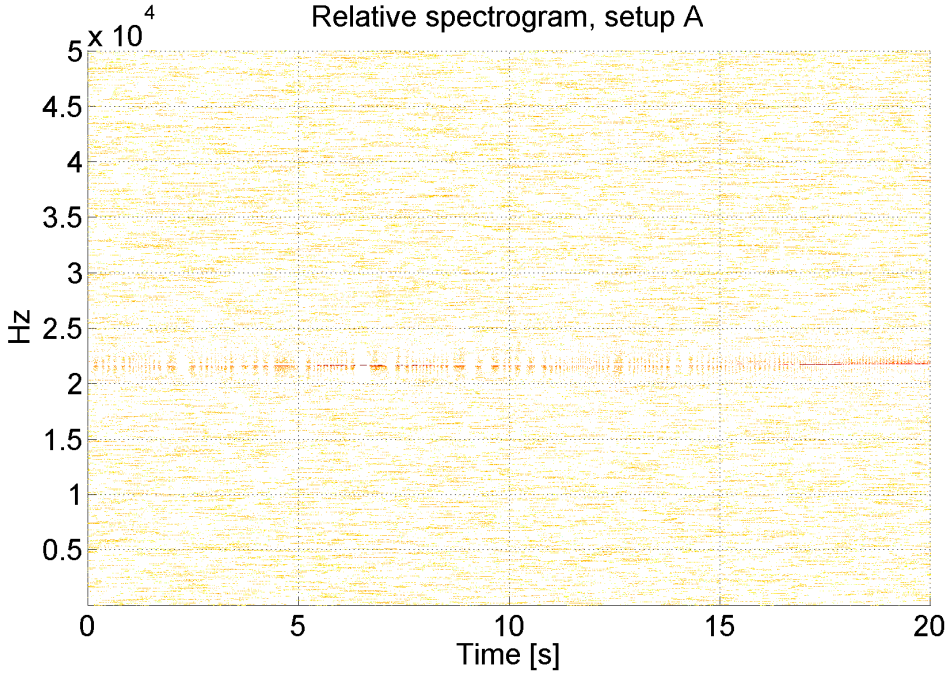

Figure 20: *Relative Spectrogram of the received signal. No signs of* 1*s long periodic disturbances of any kind.*

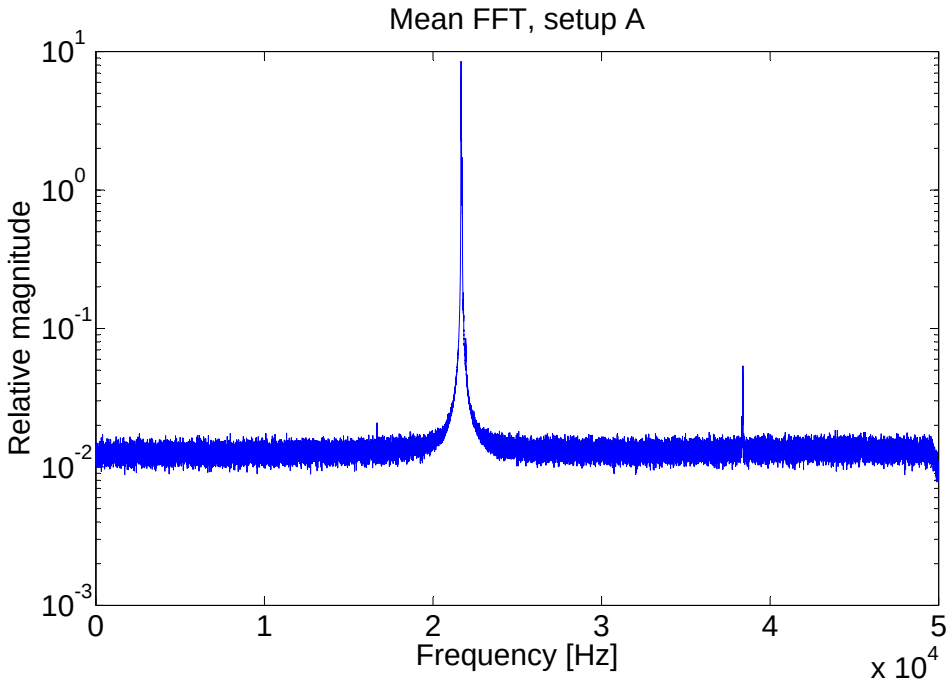

Figure 21: *The means of all FFTs in the spectrogram in figure 19.*

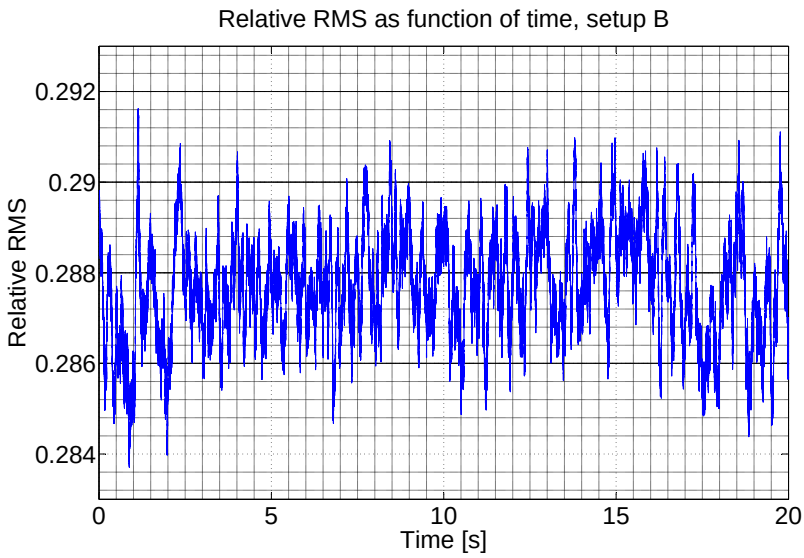

Figure 22: *Plot of the received signal's RMS in time domain. No signs of* $1s$ *long periodic disturbances of any kind.*

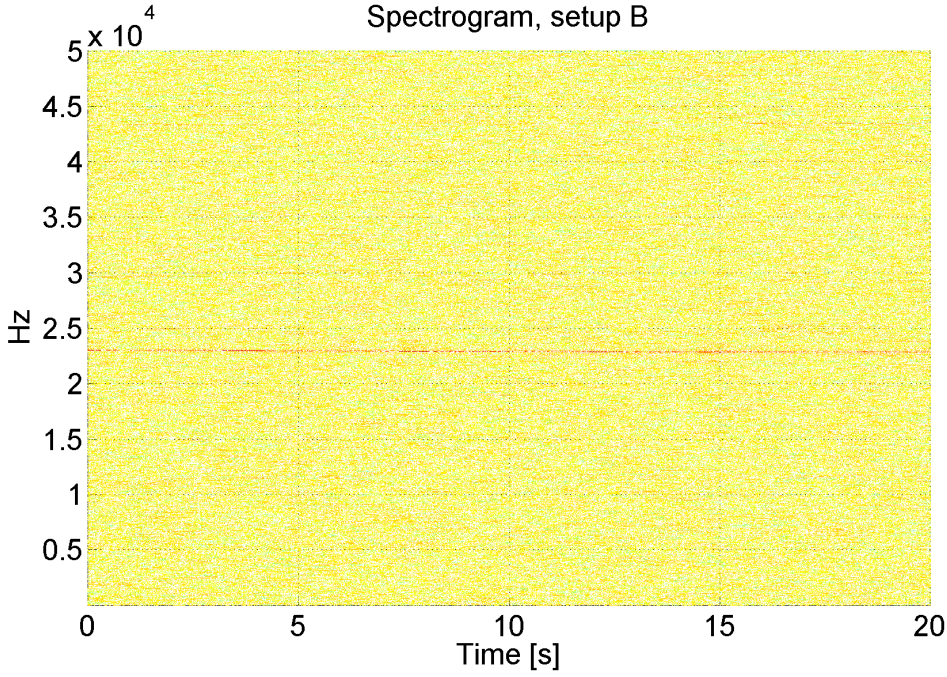

Figure 23: *Spectrogram of the received signal. No signs of* 1*s long periodic disturbances of any kind.*

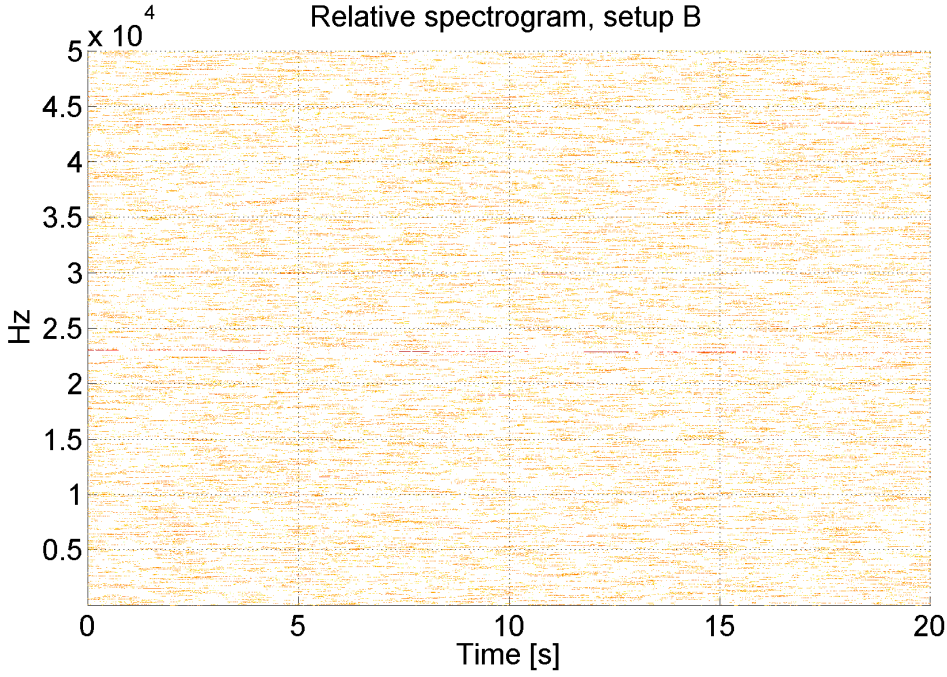

Figure 24: *Relative Spectrogram of the received signal. No signs of* 1*s long periodic disturbances of any kind.*

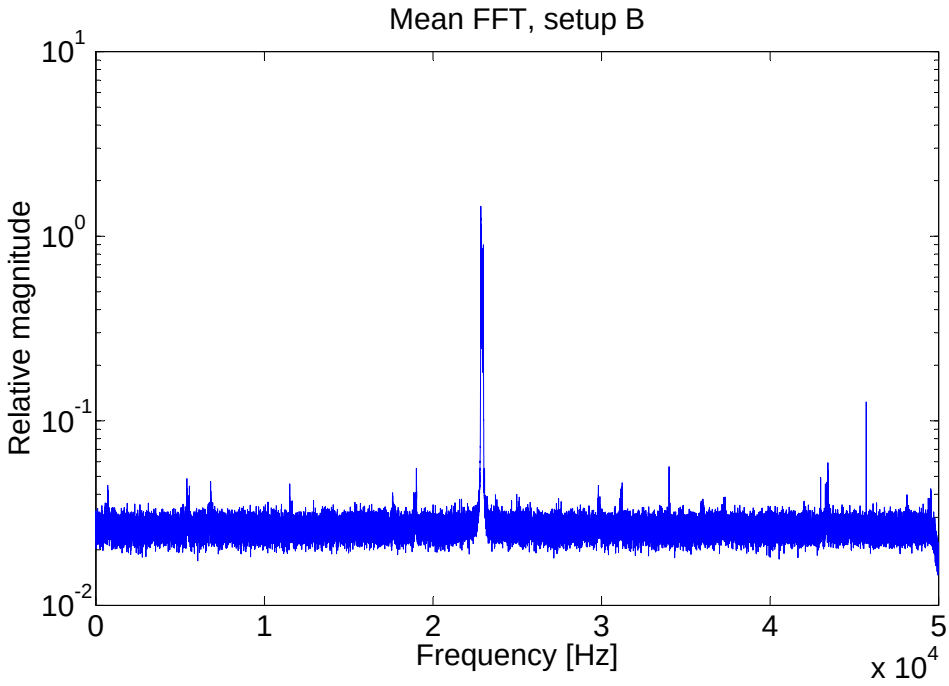

Figure 25: *The means of all FFTs in the spectrogram in figure 19.*

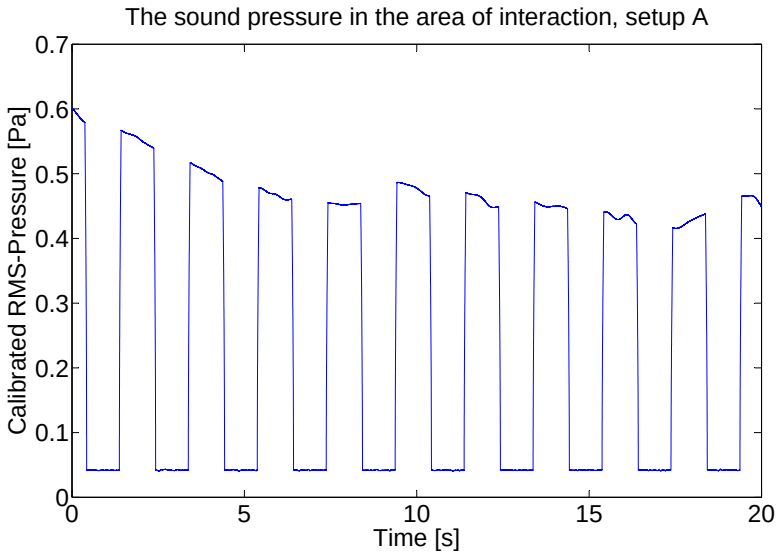

Figure 26: *The gliding RMS in the point of interaction between acoustic- and electromagnetic waves. Setup A, 20640Hz.*

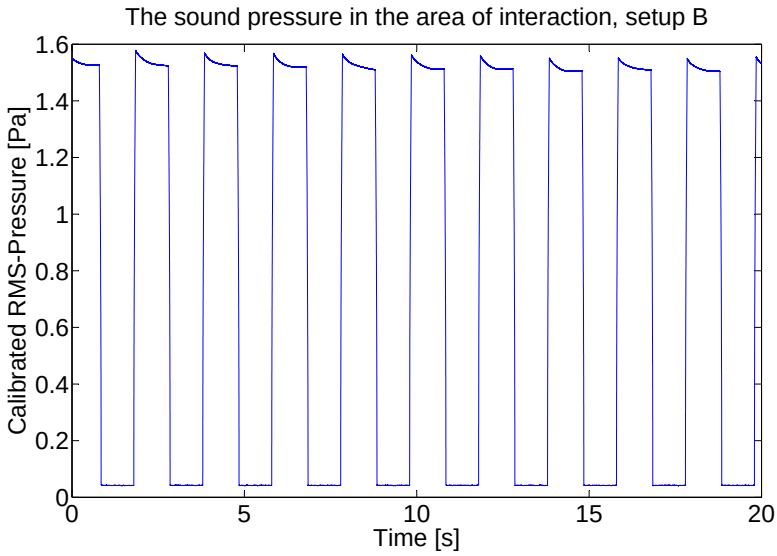

Figure 27: *The gliding RMS in the point of interaction between acoustic- and electromagnetic waves. Setup B, 12800Hz.*

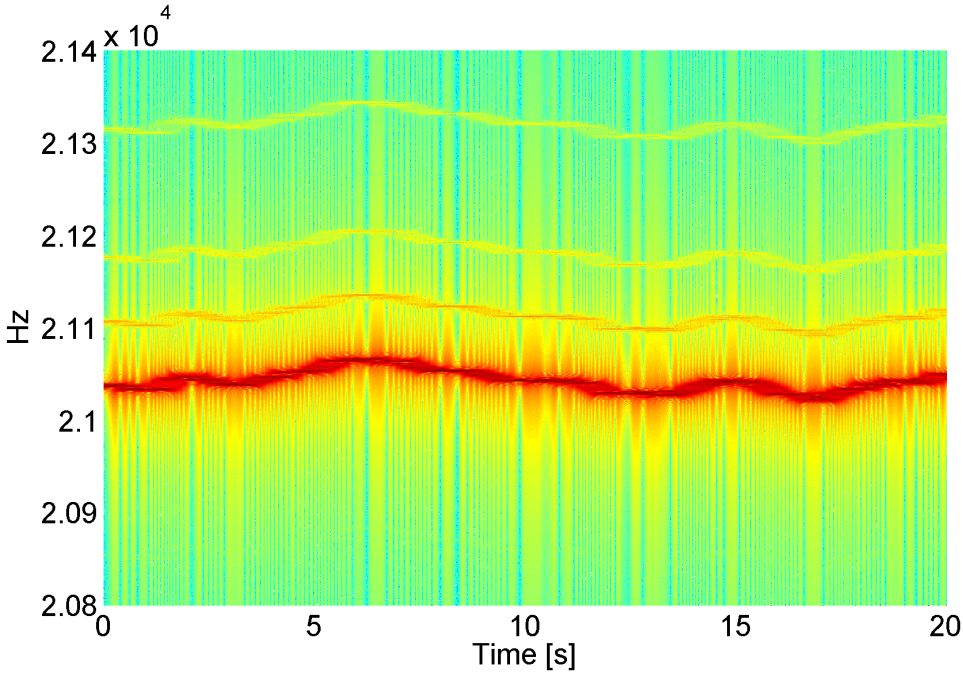

Figure 28: *Spectrogram of the received signal, with acoustic source turned off. Measurement done with equipment placed like in setup B.*

8 Discussion

8.1 Equipment Verification

8.1.1 Acoustic Equipment

The acoustic source is directive at $12.5kHz$(Figure 12) and even more so at $20.5kHz$(Figure 13), with beam widths being $\approx 30°$ and $\approx 25°$, respectively. Also, the acoustic sources frequency response (Figure 11) is high enough at both $12.5kHz$ and $20.5kHz$, with only $\approx 5dB$ difference in power at the two frequencies. Since the system runs on one frequency at the time, the level difference should not be of much importance other than that the acoustic source is capable of producing a sufficiently high level for the bistatic RASS to work.

According to 2.1, the power of the acoustic field is proportional to the power of the scattered EM-wave, thus insufficient acoustic power will cause any forward scatter to be indistinguishable from the EM background noise. However, any acoustic power (at the Bragg frequencies) should produce a forward scatter to some extent.

8.1.2 Radio Equipment

The simple receiver, paired with a simple dipole antenna, does pick up significantly more signal at the frequency at which the transmitter is sending on, confirming that the receiver does work. Comparing the two FFT plots, figure 15 and figure 16, it is apparent that the SNR for the received signal is $\approx 24dB$.

When assuming that the RASS forward scatter will be at another frequency (due to doppler shifts because of the sound speed), any forward scatter being stronger than $-24dB$ should be visible with this setup. $24dB$ translates to the noise power being $\approx \frac{1}{251}$ of the signal power. Hence, to be able to detect any forward scatter the magnitude of the scattered power have to be at least $\frac{1}{251}$ of the transmitted signal, when assuming that this exact setup is used. When replacing both antennas by directive horn antennas (Figure 17), the SNR reads $\approx 40dB$, or 10000. For a scatter to be detectable with this setup, it has to be stronger than 0.1‰ of the transmitted power.

8.2 Bistatic RASS

Forward scattered signals at around $40.6kHz$ and $32.8kHz$ were expected on setup A and B, respectively (4.3). When studying the spectrograms, figures 19 and 23, there does not seem to be anything at all that correlates to the burst

RMS, figures 26 and 27. When processing the data further and plotting the differential between the spectrograms and the mean FFT plots, the correlation is still visually absent.

The mean FFT plots and the spectrograms clearly displays the direct transmission as a peak at $\approx 23kHz$. Comparing the mean FFT plots at setup A and setup B, this direct transmission is weaker for setup B. The antennas are placed closer in setup B compared to setup A, reducing the angle between them. This is probably the reason for the difference in directly transmitted power.

8.2.1 Acoustic and Electromagnetic Observations

Comparing to the differences in absorption calculated in 4.4 and the acoustic sources frequency response (11), the difference in SPL should be

$$0.3dB(abs) + 4dB(freq.) \simeq 4.3dB$$

at $2m$ from the source. The measured SPLs (7.2.2) at $2m$ differs by $\approx 10dB$, $5.7dB$ of which can not be accounted for by difference in absorption. This may be due to the frequency response of the measurement chain.

The observed variations and deviations in received frequency, compared to the source settings, may be caused by inaccurate oscillators or re-sampling. The stable frequency deviation is taken into account when discussing the result, and the variation in frequency is $\leqslant 100Hz$, much smaller than the frequency of the Doppler shifts to be detected ($f_d \in (12, 21)kHz$). Hence, for this system the inaccuracies in frequency should not be a problem.

8.3 The System in conjunction with meteorological Measurements

GNU Radio and USRP2 radio transceivers provided quite good frequency measurements when post processed with Matlab. When considering using the system in conjunction with wind measurements, the frequency resolution is of paramount importance as it will increase resolution on measured Doppler. Using a downsized system within a anechoic chamber provided the possibility of controlling temperature, wind and humidity.

9 Improvements to the Test Setup (Future work)

Although the experiment failed to detect any scattered signal, the system at hand has been thoroughly tested and documented. This makes it possible to suggest concrete improvements to the existing system. It is also possible to compare the results of any changes to this system by the measurements done to prove/disprove if any improvements were made.

9.1 Connecting Radios and acoustic Source

Being able to couple the acoustic- and electromagnetic sampled signals in time will increase the certainty of the measurements. A trigger signal, or recording both signals simultaneously in a stereo track will make it possible to use cross correlation between the two.

An approach may be to forward the sampled (and decimated) signal from the USRP2 to the HD recorder. The main disadvantage of this approach is that the computer's DACs are far inferior with respect to SNR and linearity. The use of an external sound card may reduce this problem.

The other approach is to include a trigger signal, which is recorded on both the acoustic and the electromagnetic recorders. This may be a source that emits both a loud noise and a electromagnetic pulse at the same time. This pulse can then be identified on the recordings later, and provides a t_0 which can be used for synchronizing the independent recordings. The main advantage to this method is that one does not need to use the computer sound card, and that different sampling frequencies for the acoustic and electromagnetic signals may be used. The major drawback is that synchronizing the two recordings represent additional work.

9.2 Enhancing acoustic Power and using Frequency Sweeps

The power of the scattered electromagnetic wave is a function of the acoustic power. To achieve increased acoustic power one, or several of the following can be done:

1. Replace the acoustic source for one more directive or with higher sensitivity.
2. Increase the voltage over the acoustic source.
3. Fit more than one acoustic source in an array.

Replacing the acoustic source for one more directive or one with higher sensitivity will increase the acoustic power. The main disadvantage is that the potential for gain is very low, as the acoustic source already is both quite directive and has relatively high sensitivity.

Increasing the voltage over the acoustic source may be done. During the measurements, the voltage was $38.5V_{P-P} = 13.6V_{RMS}$, translating to a power of $30.9W$ when assuming an impedance of 6Ω. The power amplifier was set to maximal amplification, so to achieve higher power the voltage of the input signal to the power amplifier should be increased. As to the acoustic source itself, it can handle up to $90W$.

The power amplifier can clearly handle higher power output, and connecting more acoustic sources in parallel will increase the overall acoustic power and may also help increase directivity as the aperture size is increased. Sweeping the acoustic source may be a good addition to the system described. The advantages of a sweep being that all frequencies within a range may be tested in a time-effective way. The main disadvantage is that at a point in time, there is more than one frequency and wavelength present in the area of interaction between the acoustic and electromagnetic field.

9.2.1 Enhancing Radio transmitting Power and reduce direct Transmission

For improving the signal to noise ratio, the transmitting power can be increased. In general there are three ways to enhance the transmitting power of this system, namely to

1. Fit a more directive antenna.
2. Fit a power amplifier between the USRP2 and the antenna.
3. Replace the transmitting USRP2 with a different transmitter.

A more directive antenna may be a very preferable improvement to this system. One of the reasons being it will increase the amount of power transmitted in the "right" direction, thus improving the signal to noise ratio. It will also reduce the power transmitted along the line of sight between the two antennas. This will help distinguishing reflected received signal from directly transmitted signal, and thus make it easier to identify correlation between acoustic bursts and the amplitudes on the RMS plots(Figures 18 and 22).

A power amplifier fitted between the USRP2 and the antenna will increase the transmitting power of the transmitter, provided the output is greater than

that on the USRP2 and that the impedance matching between USRP2 and amplifier, and amplifier and antenna, is sufficiently good. A wide variety of commercially available amplifiers exists.

The transmitting USRP2 may be replaced by a completely different transmitter. A power amplifier and a signal generator may serve as a fully functional transmitter for the purpose. Taking into account that the transmitter only has to work on a single frequency, making one from scratch should be simple.

10 Conclusions

10.1 Equipment verification

The acoustic system was proved to operate on a suitable frequency area, with sufficiently flat frequency response. Also the acoustic source was found to generate a sufficiently narrow beam at the frequencies tested. The microphone and recorder were found to have very little frequency dependence on the frequencies in question. Hence the acoustic equipment is suitable for the experiment on RASS.

The Ettus Research USRP2, paired with a horn antenna, is a versatile and directive radio transceiver. Among the functions are real time on-screen FFT, software mixers and the ability to write samples directly to a file. This, and the ease of making, and altering transceiver programs makes it well suited for an experimental RASS.

10.2 Bistatic RASS

Two bistatic RASS were implemented within a anechoic chamber. None of the systems detected any sign of Bragg-scatter. Insufficient acoustic or electromagnetic power are both reasonable reasons for failing to detect the scatter. As to whether any scatter is present at all, is inconclusive.

Although no Bragg-scatter were detected, other important parameters such as acoustic power and SNR were measured. Considering this implementation a benchmark system, future implementations should seek to increase the scattered power, either by increasing transmitted radio power or by increasing acoustic power in the area of interaction.

When considering the system for use in conjunction with wind measurements, the resolution in frequency and time makes it easy to accurately detect and measure the Doppler of the scatter. Additionally, the use of an indoors anechoic chamber provides a very well controlled environment with respect to wind, temperature and humidity.

Hence this system, with modifications yielding increased scatter, should be well suited for a system exploring the impact of meteorological parameters on a RASS.

References

[1] Nikoleta Jones, Chrisovaladis Malesios, and Iosif Botetzagias. The influence of social capital on willingness to pay for the environment among european citizens. *European Societies*, 11(4):511–530, 2009. doi: 10.1080/14616690802624168.

[2] S. Raghavan. *Radar meteorology*. Atmospheric and oceanographic sciences library. Kluwer Academic Publishers, 2003. ISBN 9781402016042.

[3] Andreas Øvstebø. Radio-acoustic sounding system for low velocity wind measurements; acoustical considerations, 2011.

[4] D. T. Gjessing, R. Hansen, and J. Saebboe. Characterisation of wind field with high resolution in time and space by the use of electromagnetic and acoustic waves. *Radar, Sonar and Navigation, IEE Proceedings, vol. 148*, 2001.

[5] Jone Saebboe. Estimation of wind and turbulence by a radio acoustic system.

[6] Gerhard Peters. History of rass and its use for turbulence measurements. *Geoscience and Remote Sensing Symposium, 2000. Proceedings. IGARSS 2000. IEEE 2000 International*, 2000.

[7] David K. Cheng. *Field and Wave Electromagnetics*. 2nd edition, 1989. ISBN 9780201528206.

[8] George S. K. Wong and Tony F. W. Embleton. Variation of the speed of sound in the air with humidity and temperature. *Journal of the Acoustical Society of America, vol. 77, No. 5*, 1985.

[9] Graham Brooker and Javier Martinez. Low-cost monostatic radio-acoustic sounding system for indoor temperature profiling. *Radar Conference, 2008. RADAR '08. IEEE*, 2008.

[10] L. E. Kinsler, Austin R. Frey, Alan B. Coppens, and James V. Sanders. *Fundamentals of acoustics*. 2000. ISBN 9780471847892.

[11] Ettus Research. http://www.ettus.com, 2010.

[12] *Sound Devices 722 Fact sheet*. Sound Devices. URL www.sounddevices.com/download/lit/722-facts.pdf.

[13] John G. Proakis and Dimitris G. Manolakis. *Digital Signal Processing.* 2006. ISBN 9780131873742.

[14] D.M. Pozar. *Microwave and Rf Wireless Systems.* John Wiley, 2001. ISBN 9780471322825.

A Abbreviations and Definitions

The following abbreviations are used throughout the thesis:

RASS	Radio acoustic sounding system
RADAR	Radio detection and ranging
EM	Electromagnetic
ADC	Analog to digital-converter
DAC	Digital to analog-converter
Mic	Microphone
Amp	Amplifier
GRC	GNU Radio Companion
GR	GNU Radio
FFT	Fast Fourier transform
FT	Fourier transform
DSP	Digital signal processing/processor
HD	Hard drive
RMS	Root mean squared
SNR	Signal to noise-ratio
USRP	Universal software radio peripheral
SPL	Sound pressure level

Table 4: *Technical-, or specific abbreviations used throughout this thesis. Ordinary English abbreviations are omitted.*

The following definitions are used throughout the thesis:

Bistatic (RADAR/RASS)	Meaning a system with transmitter and receiver being located at different locations
Soft radio or software defined radio	Radio that allows for changing its functionality in software.
Bragg scatter	Scatter off of a boundary/volume that satisfy the Bragg condition.
Pulse code modulation	Modulation that assigns real numbered values in accordance to the value of the signal for every sample.
Nyquist sampling theorem	States that if a signal is sampled with a sampling rate, F_s, then this signal can be restored back to the original signal without any error as long as the highest frequency in the original signal is $\leqslant \frac{F_s}{2}$[13].
Laminar/turbulent (flow)	A laminar flow occurs as a fluid flows without disruption whereas a turbulent flow consists of disrupted layers of motion.
Mixer/Mixed (signal)	A mixer is a device that multiplies two signals together. If one of the signals is a sine, the result is the other signal shifted in frequency. Hence a mixed signal is a frequency shifted signal[14].
Matlab	Computer software for mathematical computing.
WinMLS	Computer software for acoustic measurements.
frequency, f	$[f] = Hz = s^{-1}$
Electric field, $\vec{E}$	$[\vec{E}] = \frac{V}{m}$
Pressure, P, p [Pa]	$Pa = \frac{N}{m^2}$
Sound pressure level	$SPL = 20\log_{10}\left\{\frac{p}{p_{ref}}\right\}$, $p_{ref} = 20\mu Pa$. $[SPL] = dB$
Wave number, $\vec{k}$	$\vec{k} = \frac{2\pi f}{c}$
Phase velocity, c	The speed at which a single-frequency wave propagates. $[c] = \frac{m}{s}$

Table 5: *Definitions used in the thesis.*

B Matlab Scripts

```
1  function [spect, T, F, spectAvg] = ...
       computeSpectrogram100ksRelative(signal, Fs, freqFrom, freqTo);
2  % Function to compute the relative spectrogram, the difference ...
       between the mean FT and the spectrogram.
3  decimation = 1000;
4  fsamp = Fs/decimation;
5  spectrLen = 2000000; %Fixed length of 20 seconds. To avoid ...
       memory problems.
6  spect = zeros((freqTo-freqFrom)+1, ceil(spectrLen/decimation));
7  spectrogramCounter = 1;
8  for i = 1:spectrLen
9      if mod(i, decimation) == 0
10         fTrans = abs(fft(signal(i:(i+Fs-1))));
11         spect(:,spectrogramCounter)  = fTrans(freqFrom:freqTo);
12         spectrogramCounter = spectrogramCounter+1;
13     end
14 end
15 spectAvg = zeros(length(spect(:,1)), 1);
16 for i = 1:length(spect(:,1))
17     spectAvg(i) = sum(spect(i,:));
18 end
19 spectAvg = spectAvg/length(spect(1,:));
20 for i = 1:length(spect(1,:))
21     spect(:,i) = spect(:,i)-spectAvg;
22 end
23 spect(spect<0) = 0; %This line prevents negative numbers.
24 T = linspace(0, spectrLen/Fs, ceil(spectrLen/decimation));
25 F = linspace(freqFrom, freqTo, freqTo-freqFrom+1);
26 fig = figure;
27 set(fig,'units','normalized','outerposition',[0 0 1 1]);
28 surf(T,F,10*log10(spect),'edgecolor','none'); %log
29 axis tight;
30 view(0,90);
31 xlabel('Time (Seconds)');
32 ylabel('Hz');
```

Figure 29: *The function computeSpectrogram100ksRelative.m, used to create relative spectrograms. Ordinary spectrograms can be obtained by commenting out lines 15 through 22.*

```
function [levelsMe,freqsMe] = readFileGetFreqlevels(filename, ...
    frequencies)
% Function to retrieve the information from a file. The ...
    frequencies may
% not be met exactly.
fileIO = fopen(filename, 'r'); %open file for reading.
tline = fgetl(fileIO);
counter = 1;
while ischar(tline)
    if (¬isempty(tline))
        values = regexp(tline,'\t','split');
        counter = counter + 1;
    end
    tline = fgetl(fileIO);
end
fclose(fileIO);
fileIO = fopen(filename, 'r'); %open file for reading.
tline = fgetl(fileIO);
freqs = zeros(1,counter);
levels = zeros(1,counter);
counter = 1;
while ischar(tline)
    if (¬isempty(tline))
        values = regexp(tline,'\t','split');
        freqs(counter) = str2double(values(1));
        levels(counter) = str2double(values(2));
        counter = counter + 1;
    end
    tline = fgetl(fileIO);
end
fclose(fileIO);
%Then we should find the levels for the freqs we actually are ...
    interested
%in:)
levelsMe = zeros(1, length(frequencies));
indexes = zeros(1, length(frequencies));
freqNo = 1;
for i = frequencies
    freq = 0;
    counter = 1;
    while(i > freq)
        freq = freqs(counter);
        counter = counter + 1;
    end
    freqsMe(freqNo) = freq;
    levelsMe(freqNo)  = levels(counter);
    indexes(freqNo) = counter;
    freqNo = freqNo+1;
end
```


Figure 30: *The function readFileGetFreqlevels.m, used by makePolarPlots.m to sort out the data for the relevant frequencies.*

```
% A script to generate polar plots from a series of measured ...
    frequency
% responses.
frequencies = 8000:500:17500; %[19500, 20000, 21000, 22000, ...
    25000, 27000, 30000]; % Hz. Will try to find closest match.
%Reading the files:
levels = zeros(19, length(frequencies)); %Something to put the ...
    data in.
freqs = zeros(1, length(frequencies));
angles = -90:10:90;
%First the negative angle files:
for i = 1:9
    numStr = num2str(i*10);
    filename = strcat('m', numStr, '.txt');
    disp(filename);
    [levels(10-i, :),freqs(10-i,:)] = ...
        readFileGetFreqlevels(filename, frequencies);
end
%Then the positive angle files:
for i = 1:9
    numStr = num2str(i*10);
    filename = strcat('p', numStr, '.txt');
    disp(filename);
    [levels(i + 10, :),freqs(i + 10,:)] = ...
        readFileGetFreqlevels(filename, frequencies);
end
%Then the 0 degree angle file:
disp('0deg.txt')
[levels(10, :),freqs(10,:)] = readFileGetFreqlevels('0deg.txt', ...
    frequencies);


for i = 1:length(frequencies)
    %disp(freqs(1,i));
    if i ~= 0
         fig = figure('Visible','off',...
      'PaperPosition',[1 3 11 14],...
      'PaperSize',[13, 20]);
    end
    plotMe = transpose(levels(:, i));
    polar(((2*pi*angles)/360), plotMe-min(plotMe));
    grid on
    title(strcat('Beaming at f=', num2str(freqs(1,i)), 'Hz. [dB]'));
    set(gca,'Position',[0 0 1 1]);
    print(fig,'-dpdf',strcat('Beam_f', num2str(freqs(1,i)), ...
        'Hz.pdf'));
    close(fig);
end
```

Figure 31: *The function makePolarPlots.m, used to create polar plots out of the WinMLS frequency responses.*

```
function glidingRMS = computeGlidingRMS(signal, calSig)
% Function to produce a time varying RMS.

nSamples = 10000; %Samples to run the RMS over.
glidingRMS = zeros(length(signal)-nSamples+1, 1);
% Calibrator parameters:
calSPL  = 94; %dB
pRef    = 20*10^-6; %Pa
calRMS  = pRef*10^(calSPL/20); % SPL = 20log(pRMS/pREF) {DEF}
% Find the factor f, so that RMS(calSig)*f = calRMS.
calSigSqua = calSig.^2;
calSigMean = sum(calSigSqua)/length(calSigSqua);
calSigRMS  = sqrt(calSigMean);
f = calRMS/calSigRMS;

% Now we simply multiply the RMS value of the signal computed ...
    with the
% factor f to obtain the real RMS value.
progressCntr = 1;
percentage = 0;
t0 = cputime;
for i = 1:length(glidingRMS)
    theSignal = signal(i:i+nSamples-1);
    sigSqua = theSignal.^2;
    sigMean = sum(sigSqua)/length(sigSqua);
    sigRMS  = sqrt(sigMean);
    sigRMS = sigRMS*f;
    glidingRMS(i) = sigRMS;
    % To keep track of time left:
    if progressCntr == floor(length(glidingRMS)/1000)
        timeLeft = (cputime-t0)*1000;
        disp(strcat(num2str(timeLeft/60), ' minutes left.'));
    end
    progressCntr = progressCntr+1;
end
```

Figure 32: *The function computeGlidingRMS.m, used to compute the time-varying RMS values.*

C Horn Antennas used

The horn antennas have been characterized at NTNU. This is a extraction from the characterization report displaying the polar diagram.

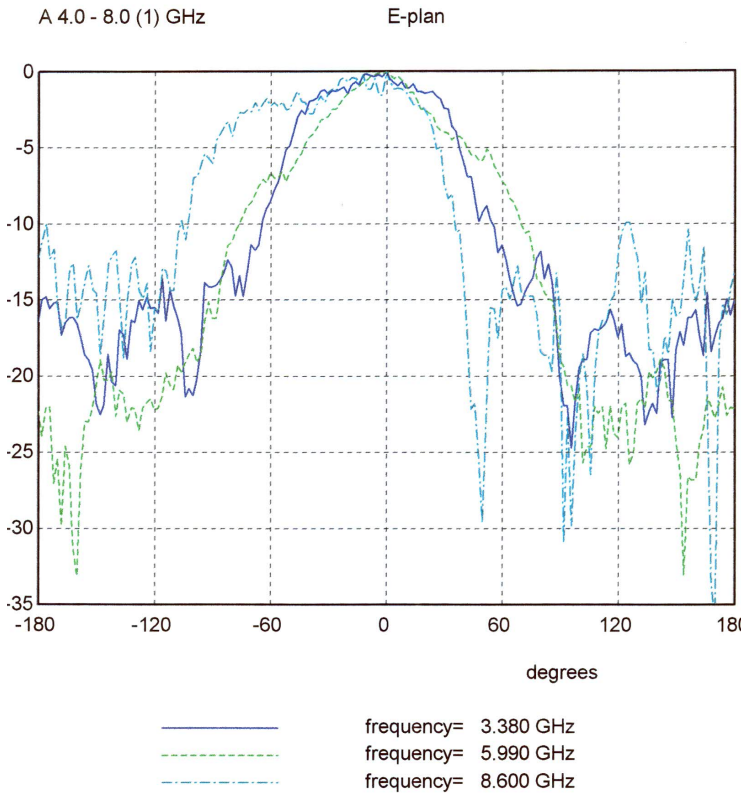

Figure 33: *The polar diagram of the horn antennas used in this thesis. The figure is extracted from the characterization report made by NTNU.*